Viscoelastic Measurements of Vocal Folds Using the Linear Skin Rheometer

***Seth H. Dailey, *Ichiro Tateya, *Douglas Montequin, *Nathan V. Welham, and †Eric Goodyer,** **Madison, Wisconsin and †Leicester, United Kingdom*

Summary: As the number of interventions for vocal fold scar grows and with the advancement of mathematical modeling, greater accuracy and precision in the measurement of vocal fold pliability will become essential. Although indirect pliability measures have been used successfully, direct measurement of tissue pliability is essential. Indirect measurement with parallel plate technology has limitations; it requires the tissue to be removed from the surrounding framework, allows no site specificity, and offers no future for *in vivo* use in animals or humans. We tested the linear skin rheometer (LSR) in the evaluation of vocal fold pliability. We measured site-specific rheology of vocal folds thereby creating "pliability maps" in human, dog, and rat cadaveric larynges under conditions of altered stiffness; the canine vocal folds possessed sulci, the rat vocal fold was stiff secondary to controlled biopsy, and the human vocal fold was injected with trichloroacetic acid. Histology was performed to confirm the site and type of canine sulci. We found that the LSR reliably detected stiffness in the vocal folds of all species and created "pliability maps" consistent with previous data and clinical observations. The LSR should prove useful in the evaluation of vocal fold pliability for *ex vivo* and ultimately for *in vivo* applications.

Key Words: Microlaryngoscopy–Viscoelasticity–Rheology–Phonosurgery–Phonomicrosurgery–Vocal fold scar.

INTRODUCTION

Vocal fold scar continues to be a challenging clinical entity in the field of Laryngology.[1] Multiple surgical treatment options including medialization thyroplasty, scar/sulcus excision, and vocal fold augmentation with collagen, fascia, and fat have all been attempted with less than optimal results.[2] Failure to achieve an optimal approach is likely based upon a lack of understanding of the fundamental nature of vocal fold scar and how to characterize it. Historically, vocal fold scar has been characterized by histologic, biochemical, aerodynamic, acoustic, stroboscopic, and rheologic parameters, including parallel plate technique.[1,3–5] Characterization of tissue rheology has been limited by technological barriers. Parallel plate technique requires excision of the entire vocal fold soft tissue away from its cartilaginous attachments and records measurements judging the multilayered vocal fold as one unit. The ability of this technique to record spatially important pliability changes is poor. Parallel plate technology cannot, for example, localize the site of the stiffness along the long and vertical axes of the vocal fold. Importantly, scarring is generally localized to the epithelium and superficial lamina propria and occupies particular sites along the long and vertical axes. This shortfall in parallel plate technology prevents precise characterization of vocal fold scar in both site and severity, limiting our ability to track focal interventions. Furthermore, mathematical modeling of vocal fold oscillation is based upon precise mapping of the vocal fold where even small tissue distortions in terms of volume or pliability will significantly alter calculations.[6–8] More precise rheometric spatial resolution will augment the power of these models. Lastly, clinical decision making is predicated upon an understanding of the tissue changes. Specifically, the site and severity of tissue volume loss and pliability loss will dictate the type of intervention to be attempted, for example, medialization for tissue volume loss versus softening of scar in an otherwise competent glottis. As the variety of interventions grows to accommodate the spectrum of problems that manifest in vocal fold scarring, a more refined characterization of the scar itself will be required to tailor the treatment to the problem. Use of the linear skin rheometer (LSR) in the characterization of vocal fold scarring addresses the shortfalls that parallel plate technology cannot.

The LSR is a precision electromechanical instrument that was designed to measure the viscoelastic properties of the stratum corneum of skin (Figure 1).[9] This measuring technique has been adapted to take viscoelastic measurements of vocal fold tissue.[10–13] The probe is attached to the tissue under test using a needle mounted at right angles to the primary axis of the rod. The rod is capable of rotating through a full circle, allowing the needle to be inserted at any angle into the tissue. The needle probe is inserted onto the vocal fold epithelium, such that the direction of motion is perpendicular to the line that can be drawn between the vocal process and anterior commissure (Figures 2 and 3). Thus, the direction of the measurement is in the same axis as the motion generated by the mucosal wave generated during phonation. The force applied is sinusoidal, with peak amplitude of 1 g applied at a rate of 0.3 Hz. Three parameters may be obtained from these curves, F_{max}, the peak force that is applied to the skin surface, P_{max}, the peak displacement occurring as a result of that force, and T, the phase shift between the two signals. The dynamic spring

Accepted for publication January 4, 2007.
This study was supported by grant ROl DC4428 from the National Institute on Deafness and Other Communication Disorders.
From the *Department of Surgery, University of Wisconsin School of Medicine, Division of Otolaryngology-Head and Neck Surgery – University of Wisconsin Hospital and Clinics, Madison, Wisconsin; and the †The Centre for Computational Intelligence - Bioinformatics Group, DeMontfort University, Leicester, UK.
Address correspondence and reprint requests to Seth H. Dailey, MD, Department of Surgery, University of Wisconsin Hospital and Clinics, Division of Otolaryngology-Head and Neck Surgery, K4/720, 600 Highland Avenue, Madison, WI 53792-7375. E-mail: dailey@surgery.wisc.edu
Journal of Voice, Vol. 23, No. 2, pp. 143-150
0892-1997/$36.00

doi:10.1016/j.jvoice.2007.01.002

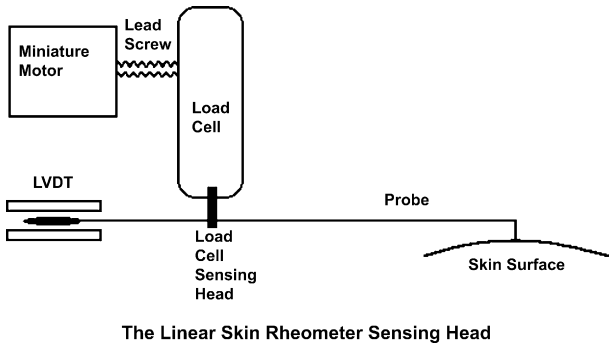

FIGURE 1. Schematic of the LSR device.

rate (DSR) is given simply by the formula F_{max}/P_{max}. Derivatives are calculated and expressed as g/mm, mm/N, and μm/g. The DSR is a nonfrequency dependent measurement of the elasticity of the material under test where a higher value denoted increased stiffness. The *LSR* software (Eric Goodyer) yields information for both the elastic and viscous qualities of the tissue.

The *LSR* has been used in preliminary animal studies to measure vocal fold tissue pliability. These studies in pig, sheep, and rabbit models showed the ability of the LSR to measure superficial vocal fold pliability and to demonstrate geographic viscoelastic differences at different depths and sites along the vocal folds.[11,12] Also, viscoelastic changes were noted under experimental conditions, suggesting that the LSR will be a sensitive, reliable tool for site-specific identification of tissue stiffness. These studies, however, did not include histologic correlations and did not specifically examine sulcus deformities. We sought to examine the utility of the LSR in the reliable detection of tissue stiffness in a site-specific manner in three different species with three different conditions of tissue stiffness.

MATERIALS AND METHODS

The study was performed in accordance with the US Public Health Service Policy on Human Care and Use of Laboratory Animals, the National Institutes of Health Guide for the Care and Use of Laboratory Animals, and the Animal Welfare Act (7 U.S.C. et seq.); the animal use protocol was approved by the Institutional Animal Care and Use Committee of the University of Wisconsin-Madison (Madison, WI).

FIGURE 2. The LSR device as used for DSR measurements on hemilarynges.

FIGURE 3. The DSR measurement setup. A custom needle probe (100 mm length, 1 mm diameter, 5 mm tapered tip) was inserted into each vocal fold region of interest, perpendicular to the plane of the vocal fold medial edge and at a depth of 1 mm. Data were collected across a matrix of 30 (6 × 5) measurement points to map variations in DSR as a function of vocal fold region. The dimension with six points was in the anterior-posterior plane: the most anterior point was placed 2 mm from the attachment of the vocal fold to the thyroid cartilage and the most posterior point was placed at the vocal process. The dimension with five points was in the inferior-superior plane: Hemilarynges were marked at the superior, mid, and inferior third positions of the vocal fold lumen surface in addition to the marking at the superior vocal fold surface and in the subglottal region.

Tissue collection and preparation

Six larynges (four canine, one rat, one human), representing six vocal fold experimental conditions (normal canine, canine sulcus vocalis, normal rat, scarred rat, normal human, human with trichloroacetic acid [TCA] exposure), were used in this study.

Canine larynges were harvested from mongrel dogs sacrificed for purposes other than this study at the University of Wisconsin School of Veterinary Medicine. Visual inspection of the harvested larynges revealed three with normal appearing vocal folds and one with bilateral sulcus vocalis. Clinical records for the dog with bilateral sulcus vocalis revealed a history of kennel cough.

The rat larynx was harvested from a Sprague-Dawley rat, 2 months after unilateral vocal fold stripping as described by Tateya et al.[1] In brief, the rat was anesthetized using a mixture of ketamine HCL (90 mg/kg) and xylazine HCL (9 mg/kg) IP, the vocal folds were visualized using a telescope, and unilateral stripping was performed using a 25-G spinal needle and microforceps. Stripping continued until the thyroarytenoid muscle was exposed. The contralateral vocal fold remained intact. Laryngeal harvest was performed after humane euthanasia *via* intracardiac injection of beuthanasia (0.22 mL/kg).

The human larynx was obtained from an autopsy case. There was no evidence of previous laryngeal disease.

All harvested larynges were frozen immediately using liquid nitrogen and stored at −80°C until experimentation. Before each experiment, the larynges were thawed overnight at 4°C and then gradually warmed to 37°C. Hemilarynges were created by sagittal section along the midline, taking care not to disturb the vocal fold attachment to the thyroid cartilage at the anterior commissure.

TCA application

The TCA was applied to one human vocal fold to examine the influence of chemical stiffening on DSR. After initial data collection under normal conditions, 1 mL of 20% TCA solution was applied topically for 2 seconds followed by saline wash. The DSR measurements were then repeated. Next, 0.3 mL of TCA solution was injected into the lamina propria through the deep to superficial layers. The injection of TCA was performed to chemically stiffen the lamina propria. Five minutes after the injection, the DSR measurements were again repeated.

DSR measurement

Hemilarynx specimens were affixed to a firm table top and kept moist with physiological saline. All measurements were made at 25°C. A custom needle probe (100 mm length, 1 mm diameter, 5 mm tapered tip) was inserted into each vocal fold region of interest, perpendicular to the plane of the vocal fold medial edge and at a depth of approximately 1 mm. Placement of the probe on the vocal folds was performed under careful visual inspection to allow for accuracy and consistency of probe depth placement. The probe tip had a sharpness that allowed it to maintain position on the vocal fold while not tearing the epithelium or lamina propria. Movement of the probe during DSR measurement followed the inferior-superior vocal fold axis, consistent with the direction of mucosal wave propagation during normal phonation. Sinusoidal force was applied at 0.3 Hz with a peak amplitude of 1 g. Resulting probe displacement was generally in the vicinity of 1 mm and therefore consistent with the range of normal tissue displacement observed during phonation. All measurements were repeated six times. No evidence of tissue damage was appreciated during or after the measurement process.

To map variations in DSR as a function of vocal fold region, data were collected across a matrix of 30 (6 × 5) measurement points in all canine and human hemilarynges except for two canine hemilarynges (one normal and one sulcus) from which data were collected across 18 (6 × 3) measurement points. The dimension with six points was in the anterior-posterior plane: the most anterior point was placed 2 mm from the attachment of the vocal fold to the thyroid cartilage and the most posterior point was placed at the vocal process. The dimension with three or five points was in the inferior-superior plane: hemilarynges with three points were marked at the superior, mid, and inferior third positions of the vocal fold lumen surface, beneath the free edge; hemilarynges with five points were additionally marked at the superior vocal fold surface and in the subglottal region.

In contrast with the human and canine specimens, the small size of the rat hemilarynx precluded more than a single measurement point on each vocal fold. Thus, a single measurement position was selected in the middle of the scarred and of the control vocal folds.

Histological analysis

The two canine vocal folds with sulcus vocalis were histologically analyzed by Elastin-van-Gieson (EVG) stain, as described by Rousseau et al.[5] In brief, the vocal fold tissues were fixed in a 10% buffered formalin solution immediately after the DSR measurement. The samples were then paraffin embedded. Ten micron-thick sections were prepared for histological examination, and EVG staining was used to identify collagen and elastin proteins.

Data analysis

Mapping of DSR variations by vocal fold region was performed as follows. The six repeated measurement values at each matrix point were averaged. Mean DSR values for each matrix point were then plotted using a contour mapping function within Sigmaplot 8.0 (*Systat Software*, Inc., Point-Richmond, CA).

The DSR measurement repeatability was calculated by dividing the standard deviation (SD) by the mean value of repeated measurements at each point. The resulting ratio, known as the coefficient of variation (CV), was averaged within subjects to yield a mean per-subject CV. These per-subject means were then averaged to yield an overall CV.

Data conversion

Conversion of the LSR (g/mm) data into loss rate values was performed as follows. Five fluids of known viscosities (centipoise, cP) were obtained (Cannon Instrument Company, State College, PA) and placed into Petri dishes at 72°F; 4 × 4-inch gauze pads were placed into the fluids to act as a scaffold. Using the LSR machine, five consecutive measurements of each fluid were performed and the average for each set of values calculated. A plot of loss rate versus viscosity was then graphed.

RESULTS

DSR in canine and normal human vocal folds

In the canine (Figure 4), DSR values were consistently higher in the anterior and posterior vocal fold regions compared with the midmembranous region. In the midmembranous region, DSR values were highest near the free edge.

In the human (Figure 5), DSR values in the posterior vocal fold region were higher than all other vocal fold regions, including those measured in the canine. DSR was highest at the vocal process, with a value of 2.78 g/mm. DSR values in the infraglottic region, corresponding to the presence of the conus elasticus, tended to be greater than those observed in the vocal fold proper.

Repeatability measures across two canine and one human samples combined yielded a CV of 4.3%.

DSR in the scarred rat vocal folds

Mean DSR values (±SD) of the normal and scarred rat vocal folds were 1.35 (±0.20) and 2.37 (±0.23) g/mm, respectively

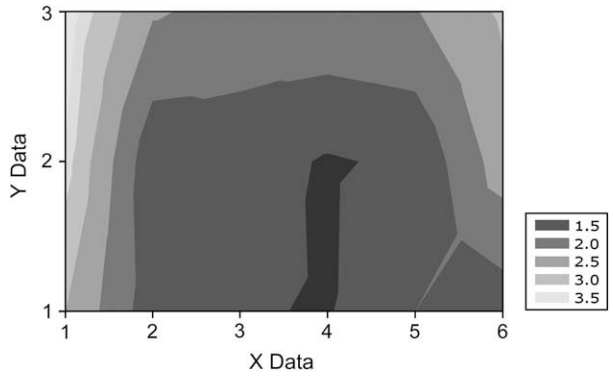

FIGURE 4. A representative 2D map of variations in DSR by vocal fold region in a normal canine vocal fold. *Y*-axis values 1, 2, and 3 correspond to measurement points on the inferior, middle, and superior third of the medial surface of the vocal fold, respectively. *X*-axis values (1–6) correspond to measurement points progressing from the anterior to posterior end of the membranous vocal fold, respectively. DSR values are consistently higher in the anterior and posterior vocal fold regions compared with the midmembranous region. In the midmembranous region, DSR values are highest near the free edge. DSR units are g/mm.

(Figure 6). The observations from the scarred vocal fold were higher than those from the normal fold.

Histology and DSR in canine vocal folds with sulcus vocalis

Although it is difficult to classify sulcus vocalis type in the canine due to absence of a vocal ligament, histological examination and gross appearance suggested the presence of a right side linear type 2 sulcus vocalis and left side pathologic type 3 sulcus vocalis[14] in the canine hemilarynges from the dog with a history of kennel cough (Figure 7). A focal lesion was observed in the superior third of both midmembranous vocal fold regions. EVG staining confirmed a deep sulcus extending to the deep layer of the lamina propria on the left, and a shallower sulcus extending to the superficial layer on the right. Both sulci were characterized by dense collagen deposition.

DSR values in the region of the left sulcus (white dashed line) were relatively higher than those in the surrounding area (Figure 5). In contrast, DSR values in the region of the right sulcus appeared consistent with those in the surrounding area. On both left and right sides, DSR values in the anterior and posterior vocal fold regions were higher than those in the midmembranous region.

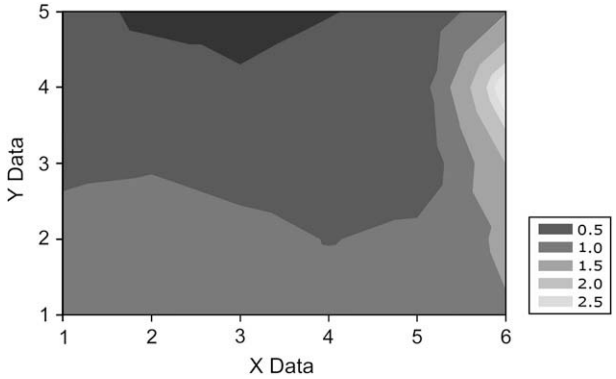

FIGURE 5. A representative 2D map of variations in DSR by vocal fold region in a normal human vocal fold. *Y*-axis values 1, 2, 3, 4, and 5 correspond to measurement points on the subglottis, inferior, middle, and superior third of the medial surface, and superior surface of the vocal fold, respectively. *X*-axis values (1–6) correspond to measurement points progressing from the anterior to posterior end of the membranous vocal fold, respectively. DSR values in the posterior vocal fold region are higher than all other vocal fold regions. DSR is highest at the vocal process, with a value of 2.78 g/mm. DSR values in the subglottal region are greater than those observed in the vocal fold proper. DSR units are g/mm.

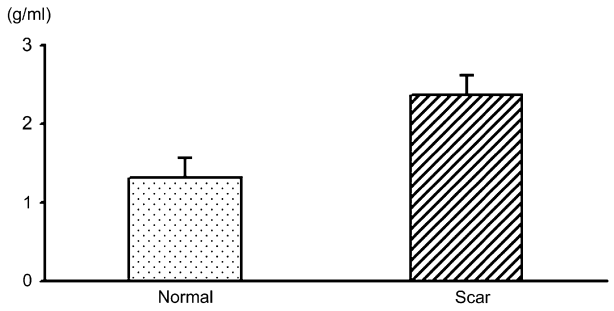

FIGURE 6. Mean DSR values of normal and scarred rat vocal folds (1.35 [±0.20] and 2.37 [±0.23] g/mm, respectively).

Effect of TCA application on the DSR value in normal human vocal folds

Before TCA application, DSR values were higher in the anterior and posterior regions of the normal human vocal fold (Figure 8). Additionally, DSR values were elevated in the subglottal region compared with the vocal fold proper. After topical application of TCA, DSR values increased across all measurement points (Figure 9). After TCA injection, DSR values further increased across all measurement points (Figure 9). After both forms of TCA application, DSR values in the anterior, posterior, and subglottal regions remained higher than those in the midmembranous region, but they increased less than the midmembranous vocal fold did (Figure 8).

Data conversion

Conversion of LSR loss rate values into values of viscosity (cP) reflected a linear relationship with a slope of 15,089 cP/g/mm (Figure 10). R^2 value = 0.9491.

DISCUSSION

The LSR device was used in this study to evaluate its reliability and sensitivity in detecting pliability values at focally specific areas in three species of vocal folds and three different conditions of stiffness. The SD of DSR repeatability values in canine and human vocal folds of 4.3% is acceptable and is similar to the values of 5% or less found by Goodyer et al.[11] The "pliability maps" which we developed in human vocal folds using either 18 or 30 points of measurement yielded results similar to

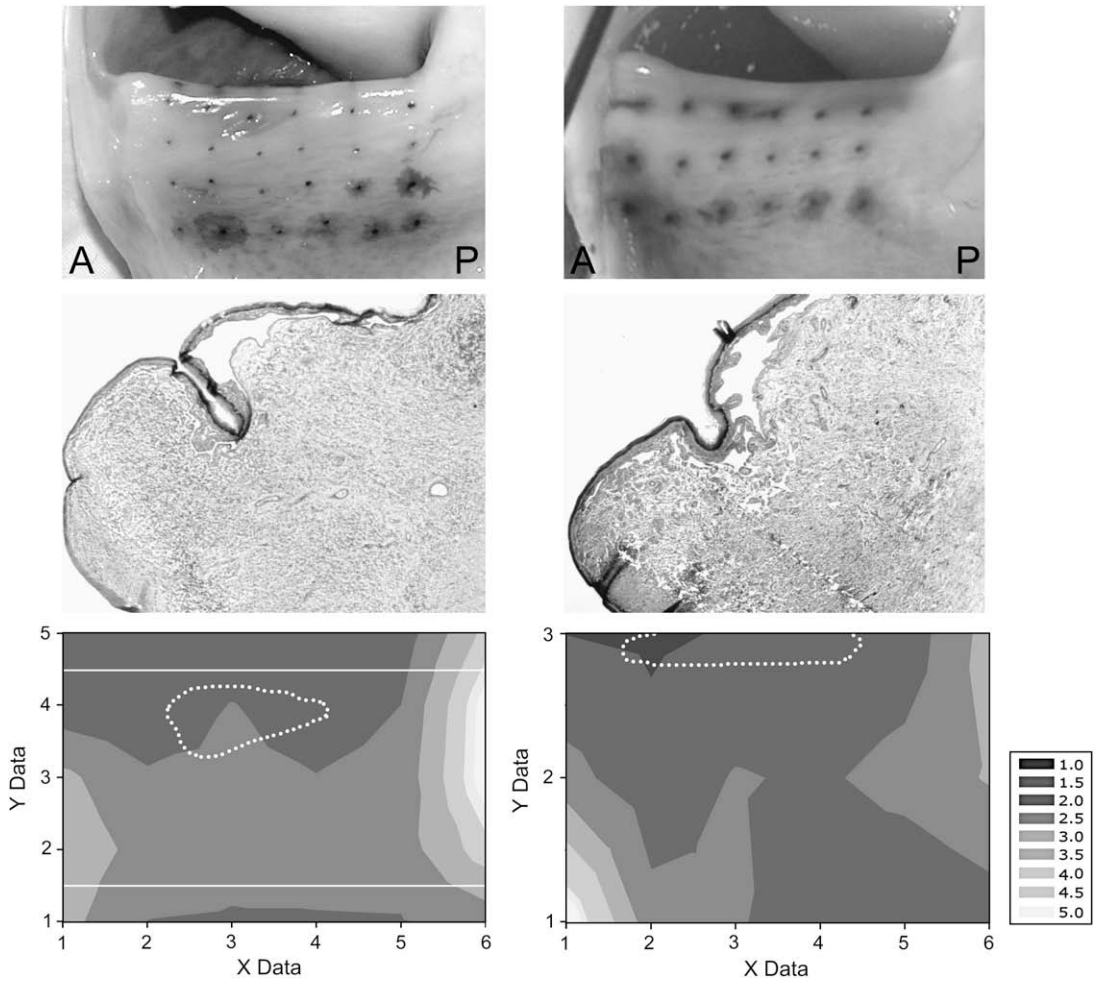

FIGURE 7. Gross appearance (upper row), EVG stain (middle row), and 2D map of DSR value by vocal fold region (lower row), in canine vocal folds with bilateral sulcus vocalis. Gross appearance and 2D DSR map of the left vocal fold are flipped horizontally. *Y*-axis values 1, 2, 3, 4, and 5 of the left vocal fold correspond to measurement points on the subglottis, inferior, middle, and superior third of the medial surface, and superior surface of the vocal fold, respectively. *Y*-axis values 1, 2, and 3 of the right vocal fold correspond to measurement points on the inferior, middle, and superior third of the medial surface, respectively. *X*-axis values (1–6) correspond to measurement points progressing from the anterior to posterior end of the membranous vocal fold, respectively. The upper and lower white lines indicate the free edge and lower margin of the vocal fold. DSR units are g/mm. (*Left*) Localized type 3 sulcus in the superior third of the left midmembranous vocal fold. DSR values in the sulcus region (white dashed line) are relatively higher than in the surrounding area. DSR values in the anterior and posterior vocal fold regions are higher than those in the midmembranous region. (*Right*) Localized shallow type 2 sulcus in the superior third of the right midmembranous vocal fold. DSR values in the sulcus region (white dashed line) appear consistent with those in the surrounding area. DSR values in the anterior and posterior vocal fold regions are higher than those in the midmembranous region.

those of previous studies in sheep and pig vocal folds.[11] These maps demonstrate the sensitivity of the LSR device to the rheologic variability in normal vocal folds. Specifically, DSR values of areas with firm tissue, such as the vocal process and the infraglottis where the fibrous conus elasticus resides, were consistently higher than the midmembranous vocal fold where thin epithelium overlies the highly pliable superficial layer of lamina propria (SLP). Stiffness increased in either direction away from the midpoint of the musculomembranous vocal fold; thinning of the superficial lamina propria and the presence of the anterior and posterior maculae flavae may help to explain this trend. Sato and colleagues have demonstrated that the area of the macula flava has an increased number of fibroblasts and is thus hypercellular compared to the relatively hypocellular SLP, likely making it more stiff.[15,16] These stiffness values correlate well with clinical observations gleaned from the palpation of different vocal fold structures during microlaryngoscopy. Of particular interest, the midmembranous segment had the lowest DSR values (the most pliable). The midmembranous segment on the medial or striking surface of the vocal fold is the most critical in voicing such that evaluation of its pliability will be clinically and experimentally critical. Aerodynamic studies have shown that the midmembranous region undergoes the highest shear stresses, likely explaining the appearance of vocal fold nodules in those with elevated subglottic voicing pressures.[17] Mathematical modeling has shown that even a tiny alteration of the configuration of this area will meaningfully affect vocal fold oscillation, confirming the importance of

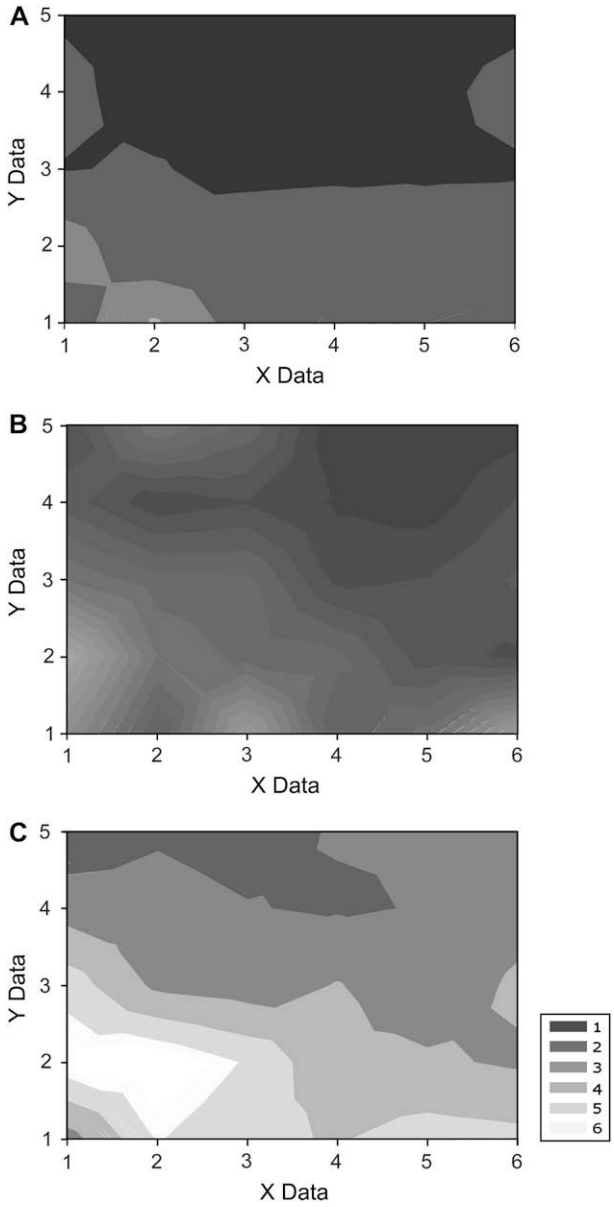

FIGURE 8. Effect of TCA application on DSR values in the human vocal fold. **A.** Pliability map before treatment with TCA. **B.** Pliability map after the treatment with topical TCA. **C.** Pliability map after the treatment with topical and injected TCA. *Y*-axis values 1, 2, 3, 4, and 5 correspond to measurement points on the subglottis, inferior, middle, and superior third of the medial surface, and superior surface of the vocal fold, respectively. *X*-axis values (1–6) correspond to measurement points progressing from the anterior to posterior end of the membranous vocal fold, respectively. DSR units are g/mm.

this region.[7,8,18,19] Furthermore, given that surgical interventions to eliminate midmembranous pathology will occasionally cause scarring and a subsequent loss of pliability, the ability of the LSR to detect pliability loss in this region will be of great utility.

As the characterization of vocal fold scarring in new experimental models must be credible, we examined whether chronic vocal fold scarring in the rat model could be reliably detected by the LSR.[20] Although the site specificity of the pliability

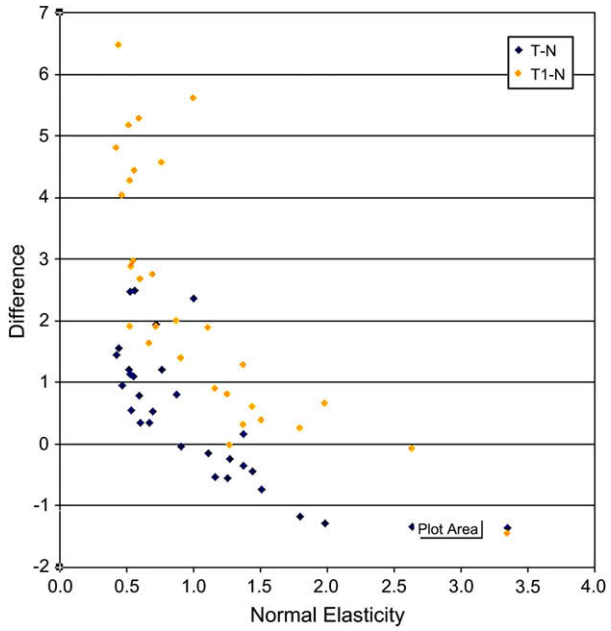

FIGURE 9. Plots of the differences in DSR values between normal and topical TCA injection (blue diamonds) and normal and topical + injected TCA vocal folds (yellow diamonds). Areas with higher pretest DSR rates (ie, stiff tissues such as cartilage) experience less alteration than areas with low pretest DSR rates (eg, midmembranous vocal fold). Values of DSR are measured in g/mm. *X*-axis is pretest elasticity. *Y*-axis is the difference in g/mm between pre- and posttest.

changes was significantly reduced due to the tiny size of the rat vocal folds, differences were found between the scarred side and the normal side, confirming our hypothesis of validity. Statistical significance was not obtained because of the small number of test vocal folds.

The LSR was sensitive in detecting this midmembranous pliability loss in all three conditions of known stiffness (TCA application/injection, sulcus, and chronic scarring). This sensitivity helps to underscore the capacity of the device to detect stiffness in both depths and sites that are relevant to the characterization of vocal fold scarring. In the human TCA application and injection models, DSR values increased across all points measured. Gray et al found that distortion of the vocal

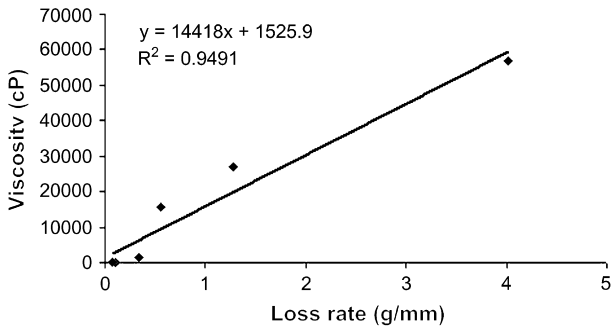

FIGURE 10. Graph of a fitted linear plot derived from measuring the loss rate of fluids of known viscosity. *X*-axis is loss rate measured in g/mm. *Y*-axis is viscosity measured in cP.

folds at the junction of the epithelial basement membrane and SLP was a common finding in benign vocal fold pathology, such as nodules.[21] Furthermore, scarring from surgical biopsies occurs at this superficial site or deeper into the SLP or beyond depending on the nature of the biopsy/procedure. That the LSR was capable of reliably detecting stiffness changes under conditions of the most superficial type (TCA topical application) and slightly deeper (SLP proper) is encouraging and supports its utility as an experimental tool. This experience correlates well with studies in calf vocal folds, in which DSR values rose with the depth of vocal fold tissue tested (eg, epithelium, SLP, vocal ligament, and vocalis muscle).[11] That the DSR values rose more in the midmembranous region than at the vocal process and in the infraglottis offers additional face validity to the application of the LSR; areas already stiff (cartilage of the vocal process and conus elasticus of the infraglottis) would not be expected to become significantly more stiff versus tissues that are innately pliable (eg, SLP). The LSR was effective in detecting stiffness changes not only under conditions of varying depth but also of varying site.

Pathologic canine vocal folds measured with the LSR device possessed focal areas of stiffness (Figure 7). These vocal folds were taken from dogs known clinically to have "kennel croup," a disease involving excess coughing and therefore transiently elevated subglottic pressures from the coughing. When excised, the vocal folds were noted to have focal areas of contraction along the medial edge, one a longitudinal scar and the other a focal scar, corresponding to sulcus vocalis types 2 and 3, respectively.[14] These visually observed findings were confirmed by histologic sectioning and staining with EVG stain, helping to corroborate these findings (Figure 7). A direct comparison cannot be made to human vocal folds because canine vocal folds do not have a vocal ligament. However, the parallel to human vocal folds is close enough to support the notion that the LSR will detect human sulcus vocalis in which site-specific stiffness changes are characteristic.[14,22]

Importantly, the ability of the LSR to detect site-specific pliability changes in experimental models opens a new door to the integration of mathematical modeling into the effects of vocal fold interventions. Berry et al have helped to pioneer modeling of vocal fold geometry and pliability to predict the outcome of biochemical and surgical procedures on voice quality.[7,8,18] This modeling has been limited to date by a lack of site-specific measures of tissue pliability. With the LSR device, correlations of modeling with aerodynamic and acoustic measures, stroboscopy and tissue histology will now be more feasible.

The correlation of loss rate to viscosity revealed a linear relationship (Figure 10). Given the multiple different units used to measure tissue pliability, including dynamic elasticity and dynamic viscosity, a linear relationship of loss rate to viscosity helps to frame the discussion and will allow for a more clear understanding in studies to come.

Although the LSR device represents an advance in direct tissue evaluation, objections may be raised to certain technical points. The needle that contacts the tissue may damage the epithelium or SLP. Tissue destruction was not observed by our group in this set of larynges. Another concern may be directed at the ability of the device to discern differences in pliability of different layers of the vocal fold. Specifically, because the needle did not penetrate the epithelium, the LSR tested the epithelium and underlying SLP as one unit and did not differentiate between the two. This objection is well founded but perhaps irrelevant because the epithelium and SLP are bound by linking proteins and oscillate as one unit *in vivo*.[21,23] Furthermore, when conditions of scarring occur superficially, the epithelium and underlying SLP scar become even *more* adherent to one another, making differentiation of epithelium from SLP unimportant. Another objection may be that the displacement of the LSR needle on the vocal fold is really testing the pliability of all layers of the vocal fold, even down to vocalis muscle and that the device is not truly testing superficial pliability changes. Given that the displacement of the needle is approximately 1 mm and that no motion of the deeper layers was visually observed during testing, we feel this concern is not a meaningful one. With the small size of the rat larynx, however, the LSR probe may have tested all layers of the vocal folds simultaneously.

Future directions for the LSR may include refinements in the test algorithms to examine whether displacements and forces applied to the vocal folds allow for more sensitive evaluations. Also, a smaller device may allow *in vivo* measurements of animal vocal folds while under anesthesia, making serial measures of pliability possible in multistage or longitudinal experiments. Furthermore, an LSR device that oscillates at physiologic frequencies may yield datasets that more accurately reflect physiologic function. Lastly, a device adapted for use in humans undergoing microlaryngoscopy has already been developed and will allow for real-time, direct measurements of tissue rheology. This capacity will improve our diagnostic abilities as well as our predictive models of surgical and biochemical interventions.

CONCLUSIONS

1. The LSR is a reliable tool for evaluation of vocal fold pliability in a research model in human, dogs, and rats.
2. Its sensitivity is satisfactory for the detection of focal stiffness in vocal folds of sufficient size.
3. Sites of focal stiffness correlate well with histologic findings of increased scar.
4. Pliability maps can now be plotted in normal, pathologic and test vocal folds with sufficient size.
5. Interventions to improve vocal fold stiffness in animal models can now be *directly* tested rather than relying upon indirect measures such as stroboscopic findings.
6. Second generation instruments are in evolution for the generation of human *in vivo* pliability maps derived during microlaryngoscopy.

Acknowledgments

We gratefully acknowledge the statistical assistance of Glen Leverson, PhD.

REFERENCES

1. Tateya T, Tateya I, Sohn JH, Bless DM. Histologic characterization of rat vocal fold scarring. *Ann Otol Rhinol Laryngol*. 2005;114:183-191.
2. Dailey SH, Ford CN. Surgical management of sulcus vocalis and vocal fold scarring. *Otolaryngol Clin North Am*. 2006;39:23-42.
3. Thibeault SL, Gray SD, Bless DM, Chan RW, Ford CN. Histologic and rheologic characterization of vocal fold scarring. *J Voice*. 2002;16:96-104.
4. Rousseau B, Hirano S, Chan RW, Welham NV, Thibeault SL, Ford CN, Bless DM. Characterization of chronic vocal fold scarring in a rabbit model. *J Voice*. 2004;18:116-124.
5. Rousseau B, Hirano S, Scheidt TD, Welham NV, Thibeault SL, Chan RW, Bless DM. Characterization of vocal fold scarring in a canine model. *Laryngoscope*. 2003;113:620-627.
6. Chan RW, Titze IR. Viscoelastic shear properties of human vocal fold mucosa: measurement methodology and empirical results. *J Acoust Soc Am*. 1999;106:2008-2021.
7. Berry DA, Clark MJ, Montequin DW, Titze IR. Characterization of the medial surface of the vocal folds. *Ann Otol Rhinol Laryngol*. 2001;110: 470-477.
8. Berry DA, Herzel H, Titze IR, Krischer K. Interpretation of biomechanical simulations of normal and chaotic vocal fold oscillations with empirical eigenfunctions. *J Acoust Soc Am*. 1994;95:3595-3604.
9. Matts PM, Goodyer E. A new instrument to measure the mechanical properties of the human stratum corneum. *J Cosmet Sci*. 1988;49:321-323.
10. Hess MM, Mueller F, Kobler JB, Zeitels SM, Goodyer E. Measurements of vocal fold elasticity using the linear skin rheometer. *Folia Phoniatr Logop*. 2006;58:207-216.
11. Goodyer EN, Gunter H, Masaki A, Kobler JB. Mapping the visco-elastic properties of the vocal fold. *Advances in Quantitative Laryngology, Voice and Speech Research*, 2003.
12. Hertegård S, Dahlqvist Å, Goodyer EN, Maurer. Viscoelasticity in scarred rabbit vocal folds after hyaluronan injection short term results. *American Academy of Otolaryngology - Head and Neck Surgery Foundation*, 2004.
13. Goodyer E, Muller F, Bramer B, Chauhan D, Hess M. In vivo measurement of the elastic properties of the human vocal fold. *Eur Arch Otorhinolaryngol*. 2006;263:455-462.
14. Ford CN, Inagi K, Khidr A, Bless DM, Gilchrist KW. Sulcus vocalis: a rational analytical approach to diagnosis and management. *Ann Otol Rhinol Laryngol*. 1996;105:189-200.
15. Sato K, Hirano M, Nakashima T. 3D structure of the macula flava in the human vocal fold. *Acta Otolaryngol*. 2003;123:269-273.
16. Sato K, Hirano M. Histologic investigation of the macula flava of the human vocal fold. *Ann Otol Rhinol Laryngol*. 1995;104:138-143.
17. Zeitels SM, Hillman RE, Desloge R, Mauri M, Doyle PB. Phonomicrosurgery in singers and performing artists: treatment outcomes, management theories, and future directions. *Ann Otol Rhinol Laryngol Suppl*. 2002;190:21-40.
18. Berry DA, Montequin DW, Tayama N. High-speed digital imaging of the medial surface of the vocal folds. *J Acoust Soc Am*. 2001;110:2539-2547.
19. Zhang Y, Jiang JJ. Chaotic vibrations of a vocal fold model with a unilateral polyp. *J Acoust Soc Am*. 2004;115:1266-1269.
20. Hirano S, Nagai H, Tateya I, Tateya T, Ford CN, Bless DM. Regeneration of aged vocal folds with basic fibroblast growth factor in a rat model: a preliminary report. *Ann Otol Rhinol Laryngol*. 2005;114:304-308.
21. Gray SD, Hammond E, Hanson DF. Benign pathologic responses of the larynx. *Ann Otol Rhinol Laryngol*. 1995;104:13-18.
22. Itoh T, Kawasaki H, Morikawa I, Hirano M. Vocal fold furrows. A 10-year review of 240 patients. *Auris Nasus Larynx*. 1983;10(Suppl):S17-S26.
23. Hirano M. Morphological structure of the vocal cord as a vibrator and its variations. *Folia Phoniatr (Basel)*. 1974;26:89-94.